Available online at www.sciencedirect.com

ScienceDirect

Energy Procedia 157 (2019) 953–965

Energy Procedia

www.elsevier.com/locate/procedia

Technologies and Materials for Renewable Energy, Environment and Sustainability, TMREES18, 19–21 September 2018, Athens, Greece

Experimental investigation and optimal power flow modelling of the first renewable microgrid in Chocó, Colombia

Edison Banguero[a], Andrés Julián Aristizábal[b*], Arslan Habib[c] and Daniel Ospina[d]

[a]*Engineering and Industrial Production Program, Universitat Politecnica de Valencia, Camí de Vera s/n, 46022, Valencia, Spain*
[b]*Department of Engineering, Universidad de Bogotá Jorge Tadeo Lozano, Cr. 4 22-61, Bogotá 110311, Colombia*
[c]*School of Automation, Northwestern Polytechnical Univeristy, 127 Youyi Xilu Xi'an, 710072, China*
[d]*Mewbourne College of Earth and Energy, The University of Oklahoma, 660 Parrington Oval, Norman, OK 73019, United States*

Abstract

This paper describes the operational performance results after one year of monitoring (2017), for the first photovoltaic (PV) micro-grid installed in Medio San Juan, Andagoya (at 5°05'34"N 76º41'43"W and 96m of altitude) in Chocó, Colombia. The renewable energy system consists of a 20 kW photovoltaic array, a three-phase grid connection inverter of the same capacity and a 132.7 kAh energy storage system. This microgrid (MG) is installed in the Renewable Energy Building of Chocó, Colombia. Power generation of the photovoltaic system and the behavior of the building's energy storage system, was evaluated by a remote monitoring system, developed through the internet. An Optimal Power Flow (OPF) model is applied to analyze the building's energy storage performance (integrated by two battery banks) and it is validated with the micro-grid performance results for each month of 2017. The results showed that the generation of altern (AC) PV- energy was 23301 kWh/year for 2017. The average of the photovoltaic system's efficiency was 11.09 %. The correlation between the OPF model results and the stored energy reported 98.79% for the battery banks.

* Corresponding author. Tel.: +57-1 242 7030; fax: +57-1 561 2107.
E-mail address: andresj.aristizabalc@utadeo.edu.co

1876-6102
10.1016/j.egypro.2018.11.262

Keywords: BIPV performance; building-integrated renewables; storage systems in buildings; power flow model; energy storage.

1. Introduction

Due to several complexities, the operators of the power systems do not have the capacity to monitor in real time when operating the electric grid and its users. Although this causes the operator to have no feedback, the objective of the Power Generation System is to provide the necessary power according to the users' needs [1].

In current power systems, electrical losses are significant in the distribution of energy, especially at low voltage levels. The reduction of losses can be achieved through the appropriate control of distributed generation resources in the distribution systems. [2]

With rapid growth of sensing, control and communication technologies in the last few decades, the power systems community has witnessed the emergence of smart micro-grids [3,4] as a viable solution to respond to the emergency situations of the main grid. A smart micro-grid [5,6] is a self-contained distributed power system that allows for high system-level energy sustainability, reliability, availability, and load support.

The term micro grid refers to a group of charges, power sources and energy storage devices [7] at low voltage levels; which can be operated as a single controllable load or a generating unit that delivers heat and power to a designated area. This concept introduces a new paradigm in order to take advantage of distributed generation in distribution grids. Therefore, a micro grid has a high control capacity and flexibility in terms of reliability and power quality of the system [8, 9].

Typically, the energy infrastructure of a micro-grid can have clean energy penetration even up to the consumer level to maintain sustainable performance. Under critical circumstances or emergency situations when the main grid is unable to meet the demand due to catastrophic failures or instabilities, a micro-grid can utilize clean as well as conventional systems for continual and reliable power generation. During the regular operation period, the micro-grids enable load sharing with main grid for efficient performance [10].

Generally, the modes of operation of the micro grids can be classified in isolated mode or connection to the electricity grid. In the isolated mode, a micro grid must be stable while it is disconnected from the main grid. In grid connection mode, the public distribution system operates as the support on which the micro grid can send / receive electrical power from / to [11].

Today, rapid advances in distributed generation technology and their benefits in modern distribution systems have made them an attractive option to the distribution companies, power system planners/operators, energy policy makers and regulators [12]. So, many efforts have been made to extend the use of MGs from several viewpoints such as: power loss minimization [13], distributed energy resource management [14,15], control and protection issues [16,17], frequency and voltage control and stabilizing MGs during islanded operation [18,19], designing advanced control strategies for smart microgrids [20-22] and reactive power planning [23].

The Transmission Companies (TransCos), however, tend to maintain standard operating conditions in terms of low transmission line congestion, high value of minimum bus voltage and low level of transmission loss, which are considered in Optimal Power Flow problems of transmission systems [24].

Many studies have been devoted to develop different models used to describe the performance of renewable energy systems and the effect of environmental conditions [25-33]. Performance results are presented for the first photovoltaic microgrid of Chocó, Colombia. In part 2 of this article, the MOPF model that was applied to our photovoltaic system is presented theoretically. In part 3 the photovoltaic micro-grid and the implemented monitoring system are described. Part 4 shows the performance results of the micro-grid during 2017 and the validation of the OPF model. Finally, part 5 presents the final conclusions for the research carried out.

Nomenclature

BIPVS	Building Integrated Photovoltaic System
OPF	Optimal Power Flow
MOPF	Multiphase Optimal Power flow
PV	Photovoltaic
MG	Microgrid

TransCos	Transmission Companies
DC	Direct Current
AC	Altern Current
YR	Reference Energy Performance
YF	Final Yield
YA	Array Yield
PR	Performance Ratio

2. Optimal power flow (OPF) methodology

This technique was developed by Carpentier in 1962 [28]. By definition, the OPF methodology is a non-linear system that consists of [29,30]:

- The objective function that should be maximized or minimized.
- The variables that must be met
- A solution methodology

In electric power systems, the OPF methodology allows optimizing a specific objective function to control the flow of electrical power without altering the established restrictions [31,32]. The OPF methodology allows establishing the ideal level of operation of the electrical system. This technique differs from its counterparts in that it must resolve the problem in the power system, working under various restrictions [34]. An advantage of this methodology is that it becomes a decision tool for power generation, transmission and distribution grids operators [35].

2.1 Problem restrictions

The problem may present some solution that must be within the limits that meet the established restrictions. The following are the inequality restrictions [36]:

- Restrictions related to the generation and consumption of alternating energy: they define the conditions of stable operation of the electrical system.
- Voltage limits: Minimum and maximum values must be established in the buses of the electric grid to guarantee the system's safety.
- Limits of electric current: due to the capacity of the conductors of the electric grid, a maximum limit of electric charge flow must be established.
- AC power flow between hybrid grids: This is the case of integration of conventional AC power with renewable energy sources such as DC photovoltaic [37].

2.2 Multiphase OPF (MOPF) model

This model allows defining a more exact approximation when using:

- Primal-dual interior point method,
- n- conductor current injection method.

In this case, the definition of the problem is [35]:

$$\min f(z); s.t.: \begin{cases} I_{Re}(z) = 0, \quad I_{Im}(z) = 0 \\ g(z) = 0, \quad h(z) = 0 \\ \underline{z} \le z \le \bar{z} \end{cases} \tag{1}$$

Defining f(z) as the objective function; I represents the total sum of current that enters the nodes of the system; g(z) and h(z) define the inequality constraints, respectively; and z represents the control variables and system state.

The Lagrange function defines as:

$$L(z,\lambda,\pi) = f(z) - \sum_{i=1}^{N} \lambda_{Im,i} I_{Re,i}(z) - \sum_{i=1}^{N} \lambda_{Re,i} I_{Im,i}(z) - \sum_{i=1}^{ni} \lambda_i \, g_i(z) - \sum_{j=1}^{nd} \pi_{j.1}\left(z_j - z_{j.min} - sl_{j.1}\right) - \mu b \sum_{j=1}^{nd} \log(sl_{j.1)} - \sum_{j=1}^{nd} \pi_{j.2}\left(z_j - z_{j.max} - sl_{j.2}\right) - \mu b \sum_{j=1}^{nd} \log(sl_{j.2})$$

(2)

Defining np as the total number of constraints and nd as the number of inequality constraints; $\lambda_{Re}, \lambda_{Im}, \pi_1 \; and \; \pi_2$ represent the dual variables; sl represents the set of imprecision variables; and μb> 0 represents the obstacle parameter.

Subsequently, the linear system is defined as follows:

$$\nabla^2 L(z,\lambda).\Delta(z,\lambda) = -\nabla L(z,\lambda) \qquad (3)$$

Defining $\nabla^2 L(z,\lambda)$ as the Hessian matrix and $\nabla L(z,\lambda)$ as the first-order derivatives of the Lagrange function.

To analyze the microgrid with the storage device, the power supplied at the common coupling point (PCC) is optimized by using a dynamic programming algorithm and the energy is assigned to the time domain. In this way, it can calculate the optimal energy management of the storage device in the mode connected to the network in buildings. Finally, the problem to intervene becomes [38]:

$$\begin{matrix} min \\ E_1 \\ \dots \\ E_M(t+dt) \end{matrix} \left\{ \begin{matrix} \Delta V\left(E_1,\ E_1(t+dt),\ E_2, E_2(t+dt), \right. \\ \left. \dots, E_M, E_M(t+dt)\right) \\ + V(t+dt, E_1(t+dt), E_2(t+dt), \\ \dots, E_M(t+dt)) \end{matrix} \right\} \qquad (4)$$

Defining V(.) in [39] and [40]; with the conditions:

Ei(t) = Ei, i = 1, 2, …, M

defining Ei(t) as the stored energy; and the cost determination ΔV is done by [40] for the intervals {t, E1(t),…, EM(t)} and {t+dt, E1(t+dt),…, EM(t+dt)}.

The expression to determine the amount of energy stored for the building:

$$\frac{d}{dt} E_i \approx \frac{E_i(t+dt) - E_i(t)}{dt}, \quad i = 1, 2, \dots, M \qquad (5)$$

3. System description

The microgrid is composed of a 20 kW photovoltaic generator installed in the roof of the Building of Renewable Energy of Chocó (CERCHOCO) Andagoya, Colombia. 80 solar panels were used, each with 250 W of power, to interconnect them and form the photovoltaic array. Fig. 1 shows the photovoltaic generator.

Fig. 1. Photovoltaic system of 20 kW installed in Andagoya - Chocó, Colombia.

Table 1 shows the data sheet of the PV modules used as photovoltaic generator.

Table 1. Electrical specification of the pv modules.

Electrical Data – STC PV MODULE	Amerisolar ASP-6P30
Nominal Maximum Power (Pmax) [W]	250
Optimun Operating Voltage (Vmp) [V]	30.3
Optimun Operating Current (Imp) [A]	8.26
Open Circuit Voltage (Voc) [V]	38
Short Circuit Current (I sc) [A]	8.75
Module Efficiency (η) [%]	15.37
Electrical Data – NOCT	
Nominal Maximum Power (Pmax) [W]	183
Optimun Operating Voltage (Vmp) [V]	27.6
Optimun Operating Current (Imp) [A]	6.64
Open Circuit Voltage (Voc) [V]	35
Short Circuit Current (I sc) [A]	7.09

The photovoltaic generator is connected to the grid using a 20 kW (STP 20000TL-US) dc/ac inverter.

Table 2 shows the STP 20000TL-US inverter's technical data.

Table 2. Technical data of the PV inverter.

Technical Data Input (DC)	Sunny Tripower 20000TL-US
Max. array power	30000 Wp STC
Max. DC voltage	1000 V
MPPT operating voltage range	150 V – 1000 V
Max. operating input current/per MPP tracker	66A / 33A
Output (AC)	
AC nominal power	20000 W
Output phases / line connections	3 / 3-N-PE
AC voltage range	160 V – 280 V
Max. efficiency	98.5%

In order to make the building energetically independent, an energy storage system with a capacity of 132.7 kAh was designed and implemented, using 48 Sunlight batteries. This energy storage system is controlled by 6 isolated ac/dc inverters. The battery bank is divided into two sets, each with 24 batteries connected in series. In Fig. 2 is possible to see the battery bank and the islanded inverters.

To the left in Fig. 2, is possible to see the PCC: where the photovoltaic generator is connected to the grid. At this point, there are several technical specifications (nominal voltage, harmonic levels, frequency range and power factor) that have to be meet according to standard IEEE 929-2000 (this standard is an electrical guideline for Colombia).

The integrated systems of photovoltaic generation, energy storage of the building and signals measurement and analysis can be seen in Fig. 3.

Due to the electrical safety aspects for the energy system and the people, the grid connection inverter must comply with the IEEE 929-2000 standard. Additionally, the inverter must comply with power quality parameters. The inverter installed with reference SMA 20 kW, meets these requirements.

Fig. 2. Installed battery bank and islanded inverters.

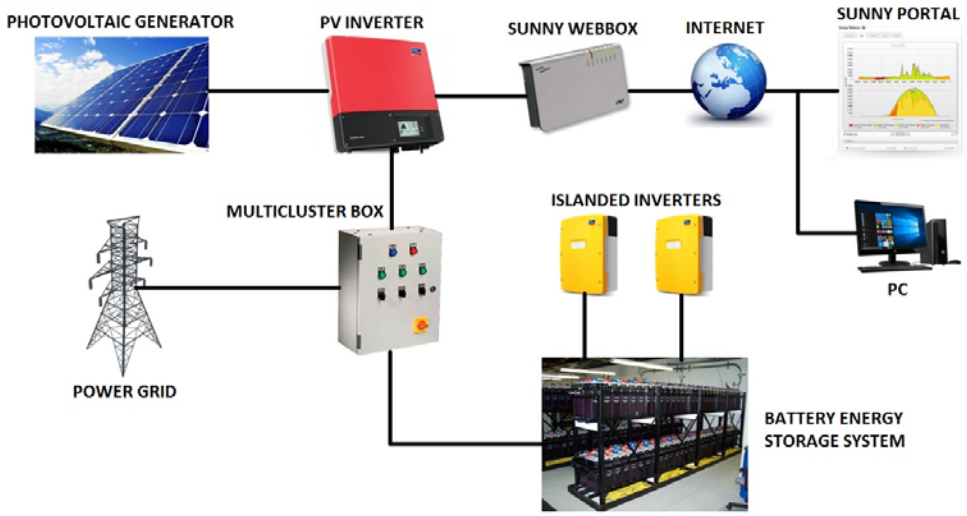

Fig. 3. Block diagram of the microgrid, including the devices of the monitoring system.

3.1 Measurement and analysis system

Using certified and calibrated sensors, one sample of the solar radiation and ambient temperature signals is acquired per second

Solar radiation is measured using a Hukseflux brand pyranometer that allows measuring global radiation between 440 nm and 1100 nm; while the ambient temperature is measured using a 10 kΩ thermistor, which allows to measure between -50 ° C to 50 ° C.

The electrical signals of the photovoltaic array and the grid inverter are transferred to the computer via the Sunny Webbox interface. This allows the transfer of system information to the Sunny Portal in the internet that allows storing, viewing and downloading information on the building's energy performance.

4. Results and discussion

4.1 Photovoltaic system performance

The production of photovoltaic solar energy at the installation site depends directly on the solar radiation and the ambient temperature. By means of the meteorological station described above, the record of these two variables was obtained, which is presented in Fig. 4.

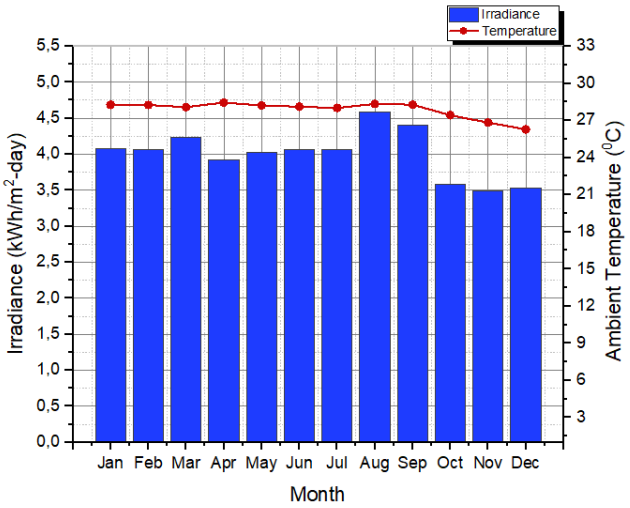

Fig. 4. Monthly behavior of solar radiation and ambient temperature in Andagoya, Chocó, Colombia for 2017.

The ambient temperature during 2017 always registered values higher than 26.83 ºC with the months of October, November and December with the lowest values. The average ambient temperature for 2017 was 27.88ºC. The ambient temperature directly affects the open circuit voltage of the solar panels.

Solar radiation presented its highest values in the months of August and September of 2017 with 4.59 kWh/m^2-day and 4.39 kWh/m^2-day respectively. Like the temperature, the lowest values occurred in the last 3 months of 2017. The annual average of solar radiation was 4 kWh/m^2-day; which represents an excellent solar potential for Andagoya, taking into account that the Department of Chocó is considered the second rainiest region of the planet and therefore there is a constant cloudiness daily. Solar radiation directly affects the photo generated current production of solar panels.

Fig. 5 shows the variation of the AC energy generated by the system versus the efficiency of the entire system for each month of 2017.

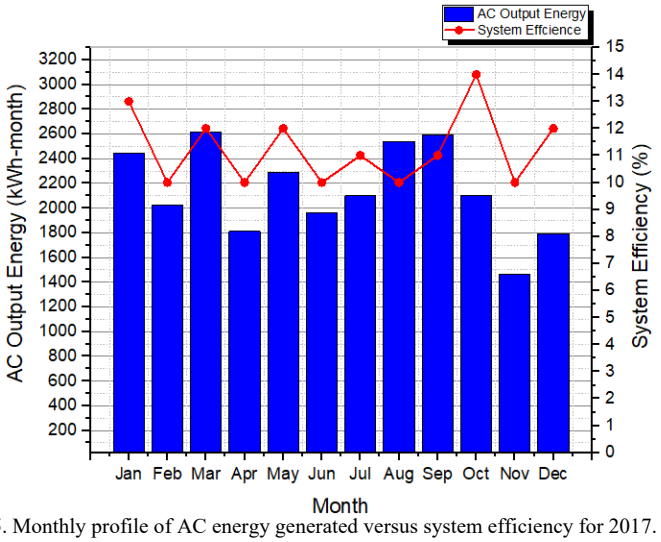

Fig. 5. Monthly profile of AC energy generated versus system efficiency for 2017.

The AC power is measured at the output of the DC / AC inverter. The variability shown in Fig. 5 is due to the changing cloudiness conditions over Andagoya and therefore the changes in solar radiation over the photovoltaic generator. The months with the highest energy production were March, August and September, with values higher than 2540 kWh/month. The month of lowest power generation AC was November with 1465 kWh/month. The average generation of AC power for 2017 was 2118.27 kWh/month.

The efficiency of the system is measured as the quotient between the AC power at the output of the dc / ac inverter and the power of the solar radiation on the photovoltaic generator. In this way, this efficiency includes the conversion losses of solar radiation to electric power of the solar panels, the losses of electric transport to the inverter and the losses of conversion of power dc to ac power by the inverter. The average value of the efficiency of the system for 2017 was 11.09%, varying between 10% and 14.2%.

Table 3 quantifies the performance variables that characterize the photovoltaic system.

Table 3.Values of: total energy produced by the PV system, parameters YR, YA, YF, LC, LS and PR.

Month-2017	AC Energy (kWh)	YR	YA	YF	LC (h)	LS (h)	PR (%)
January	2442.31	126.39	152.71	122.12	26.32	30.59	0.97
February	2024.39	113.70	136.75	101.22	23.05	35.53	0.89
March	2616.54	131.21	172.45	130.83	41.24	41.63	0.98
April	1812.35	117.65	119.97	90.62	12.33	29.36	0.77
May	2291.04	124.86	155.78	114.55	30.92	41.23	0.92
June	1966.22	122.02	138.86	98.31	16.85	40.55	0.81
July	2098.37	125.92	147.04	104.92	21.12	42.12	0.83
August	2540.51	142.35	175.83	127.03	33.48	48.80	0.89
September	2592.95	131.99	180.31	129.65	48.32	50.66	0.98
October	2101.02	110.85	140.32	105.05	29.47	35.27	0.95
November	1464.71	104.77	107.06	73.24	12.30	33.83	0.70
December	1794.20	109.56	123.71	89.71	14.50	34.00	0.82
Total		**1461.27**	**1750.80**	**1287.23**	**289.54**	**463.57**	

5.

The final yield (YF) parameter registered for the building a value of 1287.23 kWh/kWp-year. The IEA-PVPS countries register values between 700 and 1840 kWh/kWp-year [41], so this system is in this range of values of appropriate performance.

On the other hand, the reference yield YR parameter for the building registered 1461.27 kWh/kWp-year. The minimum value was measured on November with 104.77 kWh/kWp-year and the maximum was measured with August

with 142.35 kWh / kWp-year. The array yield parameter (YA) was 1750.80 kWh / kWp-year with the maximum value of 180.31 measured in September and the minimum value of 107.06 kWh / kWp-year measured in November 2017.

Finally, the PR parameter that evaluates the integral performance of the system presents a minimum of 0.70 and a maximum of 0.98 in 2017.

4.2 Photovoltaic generator performance

Fig. 6 shows the main results of the PV generator performance for 2017.

The total DC energy production of the PV array was 35016.06 kWh/year; with a mean monthly energy of 2918 kWh. March, August and September were the months with the highest DC output energy. These results coincide with a higher solar radiation recorded annually on the solar modules as shown in Fig. 4.

The average efficiency of the solar generator was recorded at 13.82% for 2017; being the lowest value of 11.98% presented in April; and the highest value of 15.22% presented in December. This behavior is a consequence of the characteristic tropical climate of Andagoya acting on the photovoltaic generator.

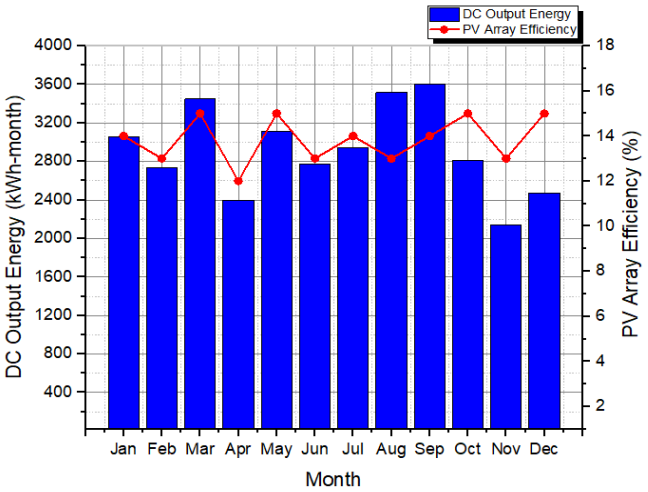

Fig. 6. Monthly profile of the DC energy versus the efficiency of the 20 kW photovoltaic generator for 2017.

4.3 DC/AC inverter performance

Fig. 7 shows the variation of the efficiency of the inverter for grid connection, calculated from the data obtained with the output voltage (Vrms).

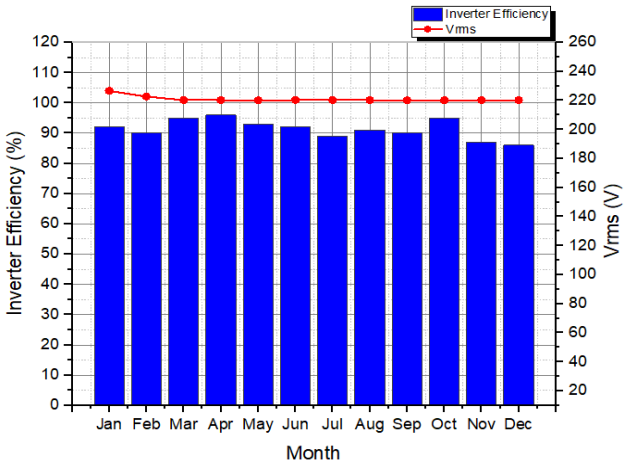

Fig. 7. STP 20000TL-US Inverter Efficiency and output voltage.

The analysis shows that the monthly efficiency of the inverter was 91.33% for 2017, with the lowest value of 86% and the highest of 96%, which indicates a photovoltaic system's correct operation achieving the maximum possible performance.

The lowest effective voltage of 220.10 V is recorded in the month of May, while the highest value recorded was in the month of January with 226.67 V. It is observed that the stability voltage always remained within the limits set by the IEEE 929-2000 standard: + 5% and -10%.

4.4 Storage energy device performance

The bank of batteries divided into two groups (B1 and B2) of 24 batteries connected in series each were monitored during each day of 2017. Figs. 8 and 9 show the input energy and the output power of each group versus the temperature internal battery.

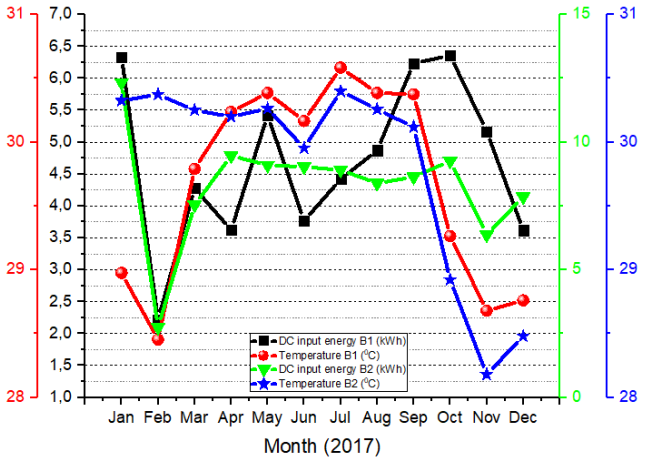

Fig. 8. Profile of the DC input power to each battery group B1 and B2 versus the internal temperature of the batteries.

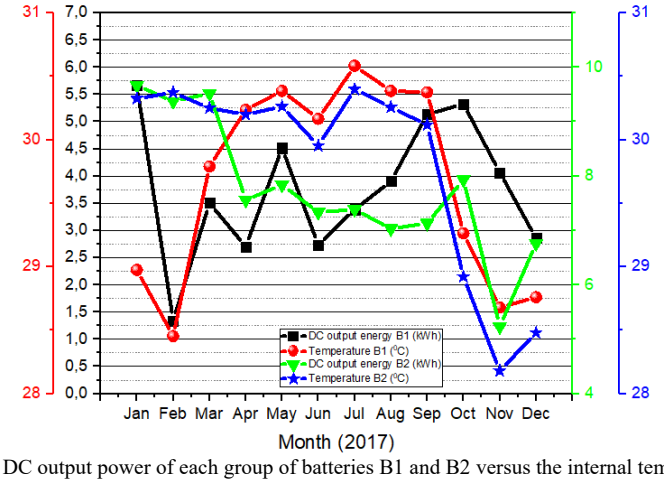

Fig. 9. Profile of the DC output power of each group of batteries B1 and B2 versus the internal temperature of the same.

Each battery group B1 and B2 has 3 Sunny Island inverters: 1 is the master and the other two are slave inverters. These inverters are responsible for managing the AC / DC power between the multicluster box and the two groups of batteries.

The DC energy stored in battery bank B2 was higher throughout the year than that of battery bank B1. The average DC power of battery group B2 was 8.30 kWh, varying between 2.74 kWh and 12.33 kWh. For battery group B1, the annual average was 4.69 kWh and varied between 2.22 kWh and 6.34 kWh. The internal temperature of the batteries registered very similar values for both groups of batteries: group B1 presented an average annual temperature of

29.67ºC while group B2 registered 29.80ºC.

Thanks to the fact that battery group B2 stored more energy throughout the year, the average energy output of this group for 2017 was 7.73 kWh, while the average power output of battery group B1 was 3.76 kWh. The energy stored in both groups of batteries was enough to increase the total load of the building, which only consists of a couple of computers and a few luminaires.

4.5 MOPF model results

The proposed MOPF model was used to evaluate the stored energy of the two groups of batteries B1 and B2 and the results observed in Figs. 10 and 11.

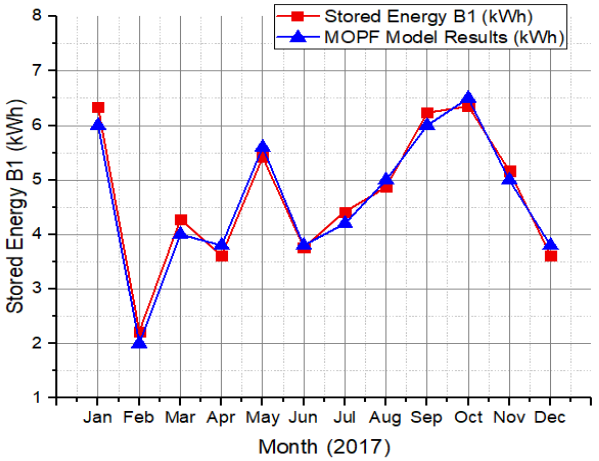

Fig. 10. Energy stored by battery group B1 vs. stored energy of the MOPF model for group B1.

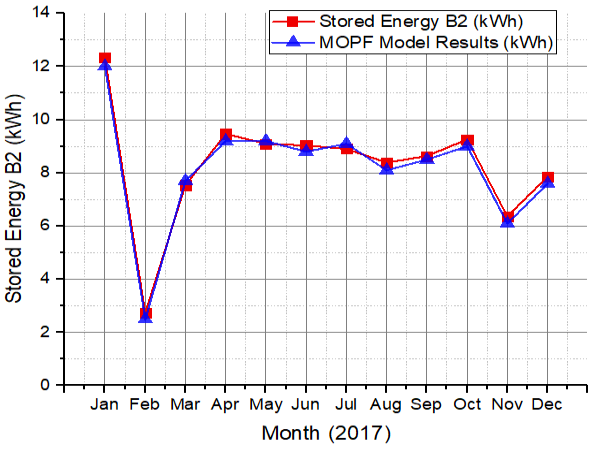

Fig. 11. Energy stored by battery group B2 vs stored energy of the MOPF model for group B2.

These results allow to validate the proposed methodology to evaluate the optimal power flow of the battery bank, since for battery group B1, the correlation coefficient between the results of the model and the values measured by the monitoring system was 98.79%; while for battery group B2 it was 97.65%. Because the model analyzes the power at the common PCC coupling point, the accuracy could be greater if the distance between the main inverter STP-20000-US and the PCC is smaller (this distance is 10m) in order to reduce losses due to voltage drop and if a cooling system could be implemented to lower the temperature of the batteries.

Acknowledgements

This work was supported by Colciencias under Grant 2013000100285.

Conclusions

From the calculations, the renewable microgrid was meant to produce 23100 kWh/year of AC power. This power generation was exceeded by 201 kWh/year for 2017.

The average solar radiation recorded in the building was 4 kWh/m2-day, exceeding the expectations in the design of the microgrid installed in the building.

The efficiency of the STP 20000TL-US was always working at the nominal values. The average for 2017 was 91.33 %. This good value contributes for an average micro grid's efficiency of 11.09 %. This last value appears to be low but it includes the PV array losses and the dc/ac inverter´s transformation.

Performance parameters YA, YF, YR, LC, LS and PR are calculated for the first time for the region of Chocó, Colombia. In conclusion, these parameters are meeting those ones reported by similar systems in Europe.

The measured parameters of the battery bank give us valuable information regarding operation of storage devices in tropical climate and under real conditions.

Based on the results shown, it is possible to conclude that the power generated by the renewable micro grid accomplish all the specifications demanded for such systems by National and International standards.

The MOPF model proposed achieved interesting results that allows to use it to model future energy backup systems for several applications. The correlation obtained was up to 98%.

References

[1] Abdi H, Beigvand S.D, La Scala M. A review of optimal power flow studies applied to smart grids and micro grids. Renewable and Sust. Energy Reviews. 2017; 71: 742-766.

[2] Bouzid AM, Guerrero JM, Cheriti A, Bouhamida M, Sicard P, Benghanem M. A survey on control of electric power distributed generation systems for microgrid applications. Renew Sustain Energy Rev. 2015; 44:751–66.

[3] Ustun TS, Ozansoy C, Zayegh A. Recent developments in microgrids and example cases around the world a review. Renew Sustain Energy Rev 2011; 15: 4030-4041.

[4] Amin SM, Wollenberg BF. Toward a smart grid: power delivery for the 21st century. Power Energy Mag 2005; 3: 34-41.

[5] Farhangi H. The path of the smart grid. IEEE Power Energy Mag 2010; 8: 18-28.

[6] Fang X, Misar S, Xue G, Yang D. Smart grid: the new and improved power grid: a survey. IEEE Commun Survey Tutor 2012; 14: 944-980.

[7] Mahmoodi M, Shamsi P, Fahimi B. Economic dispatch of a hybrid microgrid with distributed energy storage. IEEE Trans Smart Grid. 2015; 6: 2607–14.

[8] Hina Fathima A, Palanisamy K. Optimization in microgrids with hybrid energy systems – a review. Renew Sustain Energy Rev. 2015; 45: 431–46.

[9] Lidula NWA, Rajapakse AD. Microgrids research: a review of experimental microgrids and test systems. Renew Sustain Energy Rev. 2011; 15: 186–202.

[10] Hare J, Shi H, Gupta S, Bazzi A. Fault diagnostics in smart micro-grids: A survey. Ren Sust Energy Rev. 2016; 60: 1114-1124.

[11] Zhang L, Gari N, Hmurcik LV. Energy management in a microgrid with distributed energy resources. Energy Convers Manag. 2014; 78: 297–305.

[12] Ritter D, Franco J.F, Romero R. Analysis of the radial operation of distribution systems operation with minimal losses, Int. J. Elect. Power Energy Syst. 2015; 67: 453-461.

[13] Tenti P, Costabeber A, Matavelli P, Trombetti D. Distribution loss minimization by token ring control of power electronic interfaces in residential microgrids. IEEE Trans. Ind. Electron. 59 (October (10)) (2012) 3817-3826.

[14] Kumar Nunna H.S.V.S, Doola S. Multiagent-based distributed-energy –resource management for intelligent microgrids. IEEE Trans. Ind. Electron. 60 (April (4)) (2013) 1678-1687.

[15] Nayeripour M, Fallahzadeh-Abarghouei H, Waffenschmidt E, Hasanvand S. Coordinated online voltage management of distributed generation using network partitioning. Electr. Power Syst. Res. 2016; 141: 202-209.

[16] Zamani M.A, Sidhu T, Yazdani A. Investigations into the control and protection of an existing distribution network to operate as a microgrid: a case study. IEEE Trans. Ind. Electron. 61 (April (4)) (2014) 1904-1915.

[17] Kahrobaeian A, Mohamed Y.A-R.I. Interactive distributed generation interface for flexible micro grid operation in smart distribution systems. IEEE Trans. Sustain. Energy. 2012; 3(2): 295-305.

[18] Lidula N.W.A, Rajapakse A.D. MGs research: a review of experimental MGs and test systems. Renew. Sustain. Energy Rev. 2011; 15(1): 186-202.

[19] Mehrizi-Sani A, Iravani R. Potential-function based control of a MG in islanded and grid-connected modes. IEEE Trans. Power Syst. 2010; 99:

1-8.
[20] Guerrero J.M, Chiang Loh P, Lee T-L, Chandorkar M. Advanced control architectures for intelligent microgrids - part II: power quality, energy storage, and AC/DC microgrids. IEEE Trans. Ind. Electron. 60 (April (4)) (2013) 1263-1270.
[21] Guerrero J.M, Chiang Loh P, Lee T-L, Chandorkar M. Advanced control architectures for intelligent microgrids - part I: decentralized and hierarchical control. IEEE Trans. Ind. Electron. 60 (April (4)) (2013) 1254-1262.
[22] Kahrobaeian A, Mohamed Y.A-R.I. Mitigation of low-frequency oscillations in autonomous converter –based micro-grids with induction motor load. IEEE Trans. Ind. Electron. 61 (April (4)) (2014) 1643-1658.
[23] Majumder R. Reactive power compensation in single-phased operation of microgrid. IEEE Trans. Ind. Electron. 60 (April (4)) (2013) 1403-1416.
[24] Chanda S, De A. A multi-objective solution algorithm for optimum utilization of smart grid infrastructure towards social welfare. Int J Electr Power Energy Syst. 2014; 58: 397-318.
[25] Aristizábal, A.J. and Páez, C.A., 2017. Experimental investigation of the performance of 6 kW BIPV system applied in laboratory building. Energy and Buildings, 152, 1-10.
[26] Aristizábal, J. and Gordillo, G. Performance and economic evaluation of the first grid - connected installation in Colombia over 4 years of continuous operation. International Journal of Sustainable Energy, 30 (1), 34-46.
[27] A. Chica, F. Rey and J. Aristizábal. Application of autoregressive model with exogenous inputs to identify and analyse patterns of solar global radiation and ambient temperature. International Journal of Ambient Energy 2012; 33 (4): 177-183.
[28] Carpentier J. Contribution a l'étude du dispatching économique. Bull La Société Fr Des Electr 1962; 3: 431–47.
[29] Ghaddar B, Marecek J, Mevissen M. Optimal power flow as a polynomial optimization problem. IEEE Trans Power Syst 2016;31:539–46.
[30] Lin J, Li VOK, Leung K-C, Lam AYS. Optimal power flow with power flow routers. IEEE Trans Power Syst 2016:1–13.
[31] Frank S, Steponavice I, Rebennack S. Optimal power flow: a bibliographic survey I: formulations and deterministic methods. Energy Syst 2012;3:221–58.
[32] Almeida KC, Kocholik A. Solving Ill-posed optimal power flow problems via Fritz- John optimality conditions. IEEE Trans Power Syst 2016:1–10.
[33] E. Banguero, A. J. Aristizábal, and W. Murillo, "A Verification Study for Grid-Connected 20 kW Solar PV System Operating in Chocó, Colombia," in Energy Procedia, 2017, vol. 141.
[34] Vaccaro A, Canizares CA. A knowledge-based framework for power flow and optimal power flow analyses. IEEE Trans Smart Grid 2016:1–11.
[35] Radziukynas V, Radziukyniene I. Optimization methods application to optimal power flow in electric power systems. Springer Berlin Heidelberg; 2009.
[36] Abdi H, Beigvand S.D and La Scala M. A review of optimal power flow studies applied to smart grids and microgrids. Ren. and Sust. Energy Rev., 71 (2017) 742-766.
[37] Hosseinzadeh M, Rajaei Salmasi F. Robust optimal power management system for a hybrid AC/DC micro-grid. IEEE Trans Sustain Energy 2015;6:675–87.
[38] Levron Y, Guerrero JM, Beck Y. Optimal power flow in microgrids with energy storage. IEEE Trans Power Syst 2013; 28: 3226–34.
[39] Hina Fathima A, Palanisamy K. Optimization in microgrids with hybrid energy systems – a review. Renew Sustain Energy Rev 2015;45:431–46.
[40] Lidula NWA, Rajapakse AD. Microgrids research: a review of experimental microgrids and test systems. Renew Sustain Energy Rev 2011;15: 186–202.
[41] Levron Y, Guerrero JM, Beck Y. Optimal power flow in microgrids with energy storage. IEEE Trans Power Syst 2013;28:3226–34.
[42] Jahn U, Nasse W. Operational performance, reliability and promotion of PV systems. 1st ed. Germany: ISFGH; 2002.